

# A CAD-Oriented Modeling Approach of Frequency-Dependent Behavior of Substrate Noise Coupling for Mixed-Signal IC Design

Hai Lan, Zhiping Yu, and Robert W. Dutton  
Center for Integrated Systems, Stanford University, Stanford, CA 94305  
hailan@gloworm.stanford.edu

## Abstract

*A simple, efficient CAD-oriented equivalent circuit modeling approach of frequency-dependent behavior of substrate noise coupling is presented. It is shown that the substrate exhibits significant frequency-dependent characteristics for high frequency applications using epitaxial layers on a highly doped substrate. Using the proposed modeling approach, circuit topographies consisting of only ideal lumped circuit elements can be synthesized to accurately represent the frequency response using  $y$ -parameters. The proposed model is well-suited for use in standard circuit simulators. The extracted model is shown to be in good agreement with rigorous 3D device simulation results.*

## 1. Introduction

With the continued scaling of CMOS devices, system-on-a-chip (SoC) is becoming more and more interested for integrating analog, RF and digital circuitry on a single chip. Due to the conducting nature of the common substrate, noise generated by the digital circuitry can be easily injected into and propagate through the silicon substrate. With smaller and smaller headroom and more stringent requirements for analog and RF circuitry, the sensitive parts of the circuitry become more vulnerable to substrate noise. As a result, the substrate noise coupling can severely degrade the performance of sensitive circuitry.

In order to include substrate noise coupling into the design flow of mixed-signal IC's, there have been many studies into modeling of substrate noise coupling. Most numerical techniques have been based on solving the quasi-static Maxwell equation, i.e., Laplace equation [1]-[4]. In [5], a combination of finite element method (FEM) and boundary element method (BEM) is used in modeling the substrate resistance. These methods are based on fine-grid meshes or Green's function approaches and therefore are computationally intensive. Model order reduction [6] can be exploited to reduce the substrate network complexity. Scalable macro-modeling is also reported in [7]-[8]. However, most of the existing methods are

developed for low frequency applications; the frequency dependence of the substrate is largely ignored. In reality, the characteristics of doped silicon substrates exhibit frequency-dependent behavior. Detailed full-wave electromagnetic or device simulations can be performed to obtain those frequency-dependent parameters used to characterize the substrate. In [9], high frequency  $S$ -parameters are measured. However, frequency-dependent parameters are usually not compatible with standard circuit simulators. It is therefore preferable to have a CAD-oriented equivalent circuit model consisting of only ideal lumped circuit elements, which can be easily included in any standard circuit simulator, e.g., HSPICE, to facilitate mixed-signal IC design.

In this paper, a simple, efficient CAD-oriented modeling approach for frequency-dependent behavior of substrate noise coupling is proposed and validated.

First, the frequency-dependent characteristics of the silicon substrate are reviewed as a background. Second, the modeling approach is formulated. The proposed approach is then applied to two substrate noise coupling examples, where lightly and heavily doped substrates are considered. The extracted circuit models are validated with full-chip 3D device simulations. Finally, conclusions are presented.

## 2. Frequency-dependent characteristics of silicon substrate

In general the overall frequency-dependent behavior of substrate noise coupling results from various layout-dependent as well as vertical process-dependent factors, including: well-capacitances, high-low junction - capacitances, and the semi-conducting silicon substrates, etc. Since the well-capacitances can be extracted separately from the silicon bulk, this paper focuses on the frequency dependence due to the doped silicon substrate itself and high-low junction-capacitances. The resulting model can be combined with the well-capacitances to completely characterize the frequency-dependent behavior of the substrate noise coupling.

Since the silicon substrate is doped and thus semi-conducting, depending on different operating frequencies

and doping concentrations, there are three fundamental operating modes: dielectric quasi-static mode, skin-effect mode, and slow-wave mode, as qualitatively illustrated in Fig. 1 [10].

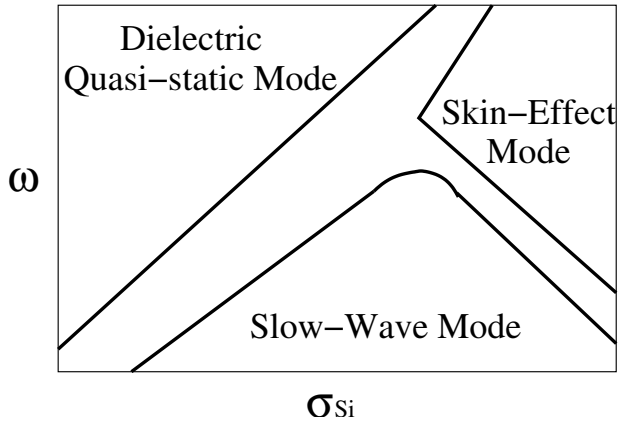


**Fig. 1. Three operating modes for silicon substrate in frequency-conductivity domain chart.**

When the frequency-conductivity product  $\omega\sigma_{Si}$  is low enough to produce a negligibly small dielectric loss angle, the silicon substrate can be treated as a dielectric. In this mode, quasi-static characterization is sufficient to model the substrate. On the contrary, when the frequency-conductivity product  $\omega\sigma_{Si}$  becomes large enough to yield field penetration into the silicon substrate, the silicon layer becomes lossy. In this mode, the electric fields and thus current flow lines tend to crowd in the skin depth region in the silicon bulk, where the skin depth is determined as  $\delta = 1 / \sqrt{\pi f \sigma_{Si} \mu_0}$ . When the frequency-conductivity product  $\omega\sigma_{Si}$  stays in an intermediate range, for example, when the frequency is not very high and the silicon conductivity is moderate, the propagating velocity slows down owing to the energy transfer across the interface associated with the dielectric dispersion and strong interfacial polarization at the silicon substrate, thus resulting in a slow-wave propagation mode. For a uniformly doped substrate, operating in any of these modes, the conductance is related to capacitance by the dielectric relaxation time constant  $C_{Si} / G_{Si} = \epsilon / \sigma$ .

### 3. Modeling approach

#### 3.1. $y$ -parameters based macro-model

A  $y$ -parameters based macro-model has been used for the 2D substrate noise coupling problem in low frequency applications [7]. However, the frequency dependent behavior and 3D layout effects were ignored in that work. This work investigates the  $y$ -parameters based macro-model extracted from rigorous 3D device simulation. The

$y$ -parameters in principle can directly provide the macro-model for substrate noise coupling analysis. However, due to the frequency-dependent characteristics of the substrate and high computational cost of performing frequency sweeping in 3D device simulation, it is more desirable to construct an equivalent circuit comprised of only ideal lumped elements, representing the frequency response.

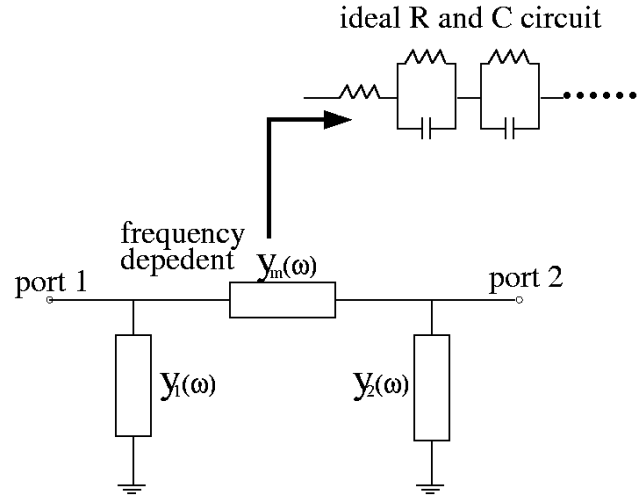


**Fig. 2. Circuit representation of  $y$ -parameters.**

The multi-port  $y$ -parameters can be reduced to the basic two-port  $y$ -parameters set. The generic circuit representation of two-port  $y$ -parameters is shown in Fig. 2. In terms of circuit elements, the two-port  $y$  parameters can be written as

$$[y(\omega)] = \begin{bmatrix} y_{11}(\omega) & y_{12}(\omega) \\ y_{21}(\omega) & y_{22}(\omega) \end{bmatrix} = \begin{bmatrix} y_{11}(\omega) + y_m(\omega) & -y_m(\omega) \\ -y_m(\omega) & y_{22}(\omega) + y_m(\omega) \end{bmatrix} \quad (1)$$

where  $y_{ij}(\omega) = g_{ij}(\omega) + j\omega \cdot c_{ij}(\omega)$ . It should be noted that the  $y$ -parameters are frequency-dependent. Moreover, for a passive two-port system:

$$y_{12}(\omega) = y_{21}(\omega) \quad (2)$$

#### 3.2. Synthesis of an equivalent circuit model

Once the frequency dependent  $y$ -parameters are obtained from device simulation, the equivalent circuit model can be synthesized in terms of a lumped circuit representation by constructing a rational function [11], [12]. The rational function has the general form:

$$F(j\omega) = \frac{A_0 + A_1(j\omega) + A_2(j\omega)^2 + \dots + A_m(j\omega)^m}{1 + B_1(j\omega) + B_2(j\omega)^2 + \dots + B_n(j\omega)^n} \quad (3)$$

A robust rational polynomial algorithm is developed to guarantee passivity. Typically, the fitting process uses Eq. (3) over a wide frequency range and leads to an over-constrained linear system of equations. The order of the final rational function largely depends on how much the data sets to be fitted vary with frequency, i.e., how much  $g(\omega)$  and  $c(\omega)$  vary with frequency, which is mainly determined by the layout geometry and specific IC process. Simulations have shown that for a typical substrate using a heavily- or lightly-doped process, second order terms of Eq. (3) should be sufficient to model the frequency response up to 100 GHz. A representative circuit model synthesized using the frequency-dependent  $y$ -parameters is illustrated in Fig. 3.

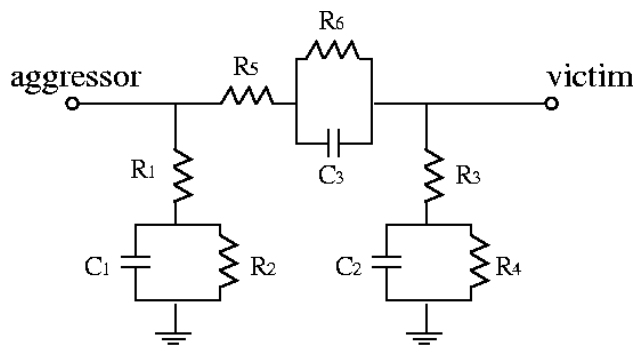


**Fig. 3. Representative circuit topography synthesized from frequency-dependent  $y$ -parameters.**

#### 4. Application examples

Two examples using a 3D full-chip model with dimension similar to that in [13] are considered here to validate the modeling approach. In order to show the significance of the frequency-dependent behavior of the substrate, the same layout is used but with different substrate configurations. Case 1 investigates the heavily doped substrate with lightly doped epitaxial layer and Case 2 studies the lightly doped substrate. The same contact layout is used as shown in Fig. 4. Chip dimensions are 3440  $\mu\text{m}$  by 3483  $\mu\text{m}$  by 10  $\mu\text{m}$ . There is one aggressor contact and one victim contact, which represents a typical digital noise source and a sensitive analog or RF circuit, respectively. Also one representative intermediate contact is placed to take into account the influence of other circuit blocks or IP blocks on the aggressor-victim pair. Both the aggressor and victim are  $p^+$  contacts with doping concentration  $N_a=1 \times 10^{20} \text{ cm}^{-3}$

and size 100  $\mu\text{m}$  by 100  $\mu\text{m}$ . The intermediate contact is  $p^+$  contact with doping concentration  $N_a=1 \times 10^{20} \text{ cm}^{-3}$ , depth 0.1  $\mu\text{m}$  and surface area 500  $\mu\text{m}$  by 500  $\mu\text{m}$ .

#### 4.1. Case 1: Heavily doped substrate with lightly doped epitaxial layer

Fig. 4 shows the substrate configuration of Case 1, where the heavily doped substrate is 6  $\mu\text{m}$  thick with doping concentration  $N_a=1 \times 10^{19} \text{ cm}^{-3}$  and the lightly doped epitaxial layer is 4  $\mu\text{m}$  thick with doping concentration  $N_a=1.2 \times 10^{15} \text{ cm}^{-3}$ .

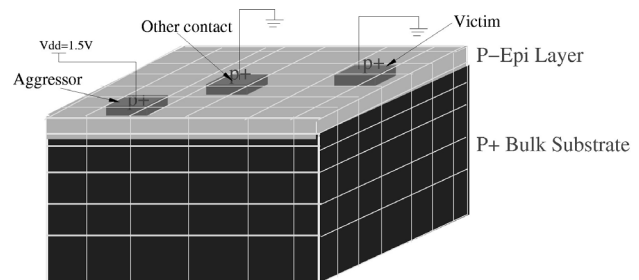
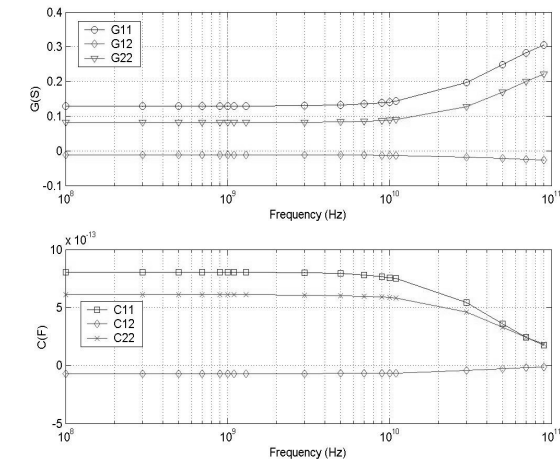


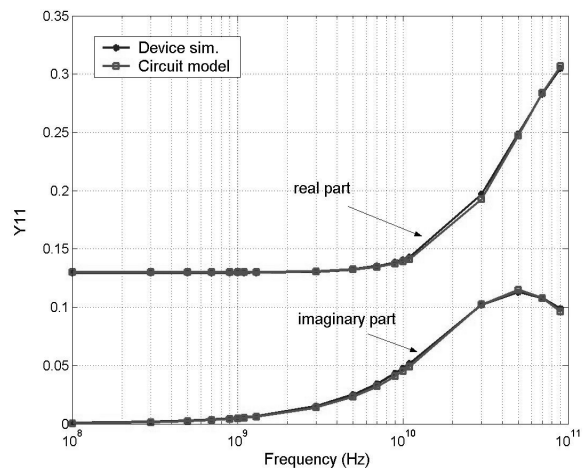
**Fig. 4. Case 1: Heavily doped substrate with lightly doped epitaxial layer.**

The aggressor contact is biased at  $V_{dd}=1.5\text{V}$  while the victim contact is grounded. The substrate back plane is floating. Note that in Fig. 4 the intermediate contact is also grounded. The  $y$ -parameters between the aggressor and victim can be obtained from 3D device simulation over a wide frequency range with the intermediate contact present. The mesh used is  $63 \times 63 \times 7$  and both electron and hole carriers are solved for.

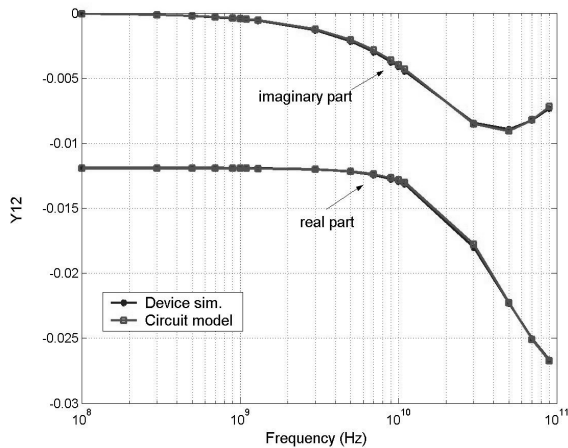
Fig. 5(a) shows the frequency-dependent self and mutual conductances and capacitances simulated with the 3D device simulator. It can be seen from Fig. 5(a) that although both the conductances and capacitances remain constant for frequencies up to around 10 GHz, they exhibit significant frequency dependence beyond 10 GHz. Note that in Case 1 there is actually no well capacitance, nonetheless the substrate shows a frequency dependence due to its lossy nature as discussed above as well as the high-low junction capacitive effects. This latter effect has been ignored in the published literature.



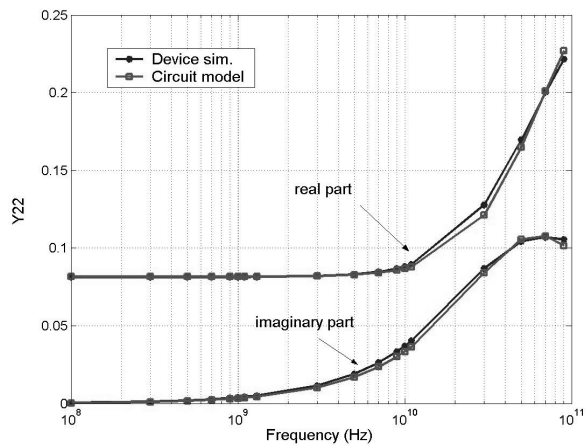
(a)



(b)



(c)



(d)

**Fig. 5. Simulation results for Case 1. (a) Device simulation results showing frequency-dependent self and mutual conductance and capacitance. (b), (c) and (d) Comparison between the circuit model and device simulations for  $y_{11}$ ,  $y_{12}$ , and  $y_{22}$ , respectively.**

**Table 1. Extracted circuit elements in case 1. All resistances in ( $\Omega$ ) and capacitances in (F)**

R1	R2	R3
2.568	4.482	3.053
R4	R5	R6
7.645	33.072	50.668
C1	C2	C3
2.010p	1.193p	0.182p

The equivalent circuit modeling approach is then applied and the extracted circuit is found to be in the form shown in Fig. 3. It should be pointed out that in fact only a few data points over the entire frequency range are needed to extract the circuit model. Therefore,

the cost of model parameter extraction is low. Table 1 lists the extracted values of the lumped circuit elements.

The resulting circuit model is included in HSPICE and then used to perform circuit simulation. Fig. 5(b)-(d) show the comparison between the extracted circuit model and rigorous 3D device simulation in terms of the real and imaginary parts of the  $y$ -parameters. Good agreement can be observed between circuit- and device-level simulations. The extracted lumped circuit model can characterize the frequency-dependent behavior of the substrate accurately, yet the computational cost is very low compared to very timing consuming device simulation. It can also be seen from Fig. 5(b)-(d) that the purely resistive substrate model is valid only for frequencies up to 10 GHz for the heavily doped

substrate with an epitaxial layer, primarily due to the frequency dependence of the high-low junction.

#### 4.2. Case 2: Lightly doped substrate

The case of using a lightly doped substrate is now discussed. The contacts are laid out in the same configuration as that used in Case 1 but the substrate is p-bulk silicon with doping concentration  $N_a=3.9 \times 10^{16} \text{ cm}^{-3}$ , as shown in Fig. 6.

Fig. 7(a) shows the device simulation results in terms of the self and mutual conductances and capacitances. It is seen that due to the less lossy nature of the lightly doped substrate, the conductance and capacitance are nearly constant-valued over a wide frequency range with only a slight frequency dependence observed at

frequencies above 80-90 GHz. Due to the low conductivity, the substrate operates in the quasi-static mode as depicted in Fig. 1.

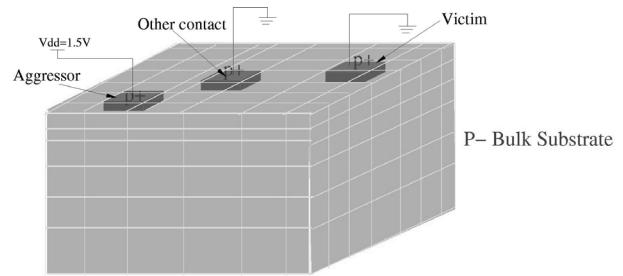


Fig. 6. Case 2: Lightly doped substrate.

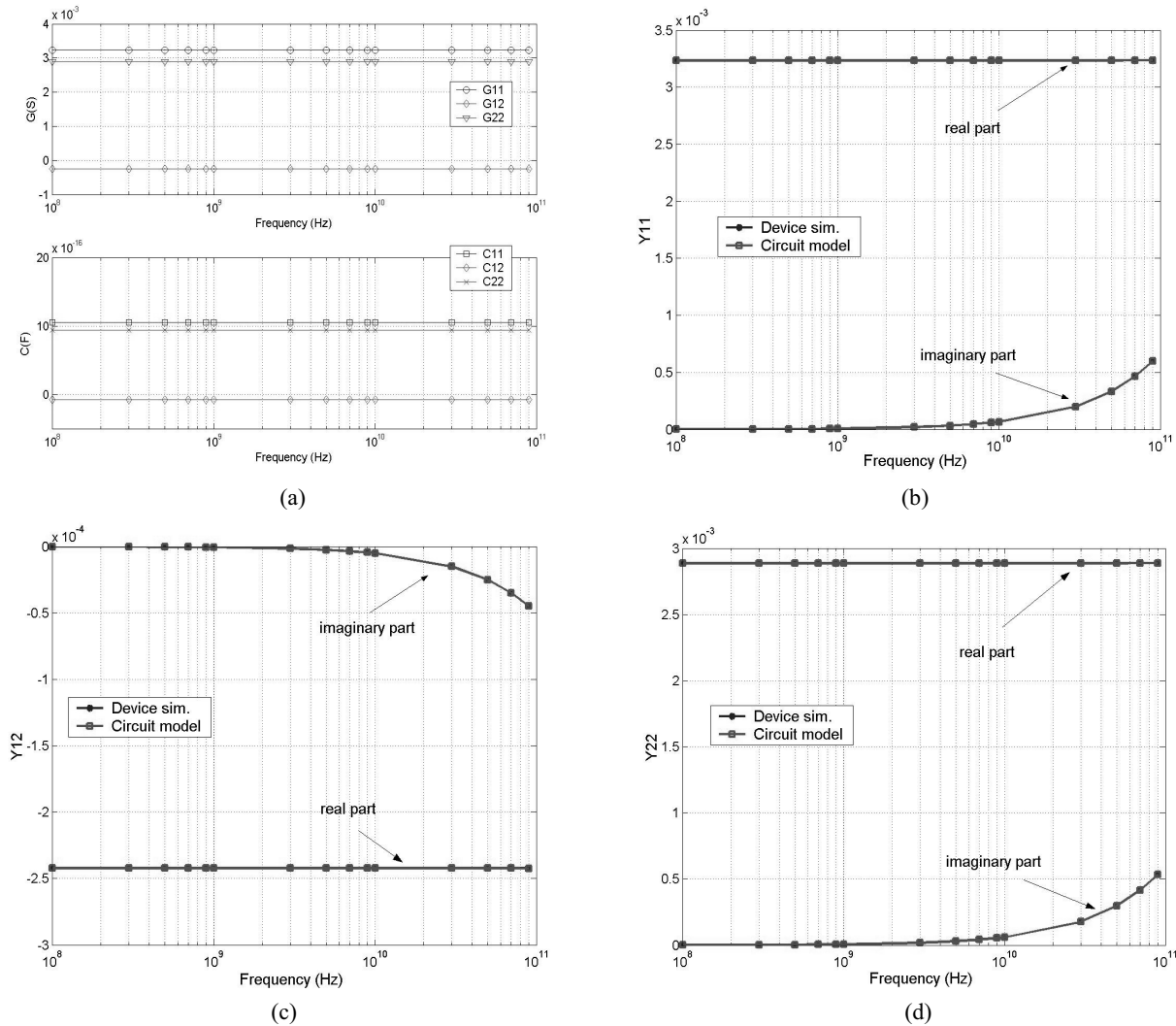


Fig. 7. Simulation results for Case 2. (a) Device simulation results showing self and mutual conductance and capacitance almost constant. (b), (c) and (d) Comparison between the circuit model and device simulations for  $y_{11}$ ,  $y_{12}$ , and  $y_{22}$ , respectively.

The generated circuit topography again follows the form of that depicted in Fig. 3. The extracted circuit element values are tabulated in Table 2.

**Table 2. Extracted circuit elements in case 2. All resistances in ( $\Omega$ ) and capacitances in (F).**

R1	R2	R3
5.133	282.544	1.484
R4	R5	R6
318.068	77.709	4.052K
C1	C2	C3
1.177f	1.033f	0.083f

Fig. 7(b)-(d) show the comparison between the circuit and device-level simulations. Again, the extracted circuit model agrees well with rigorous device simulation results. It is noted from Table 2 that the extracted capacitances are very small and as a result the displacement current path does not play a significant role until very high frequencies. Although the extracted circuit topography in Case 2 is the same as that in Case 1, the small capacitance values automatically capture the significant difference in frequency responses for heavily doped substrate and the lightly doped substrate. This further validates the generic usage of the proposed modeling approach.

## 5. Conclusions

A CAD-oriented equivalent circuit modeling approach for frequency-dependent behavior of substrate noise coupling has been developed. The physical origin of frequency-dependence of doped silicon substrate is discussed. Rigorous 3D device simulations are performed to show the frequency-dependent  $y$  - parameters. Heavily doped substrate with an epitaxial layer exhibits more significant frequency dependence than lightly doped substrate primarily due to the frequency dependence of high-low junction. A rational function approximation is used to construct the equivalent circuit consisting solely of ideal lumped elements. The modeling approach has been applied to a heavily doped substrate case and a lightly doped substrate case. In both cases, good agreement is observed between the circuit model and detailed device simulations. The proposed model can be readily included in any standard circuit simulator and should be useful in efficient simulation of frequency-dependent characteristics of substrate noise coupling in mixed-signal IC design.

## 6. Acknowledgements

This research was supported by DARPA under the NeoCAD project.

## References

- [1] R. Gharpurey and R. G. Meyer, "Modeling and analysis of substrate coupling in integrated circuits," *IEEE J. Solid-State Circuits*, vol. 31, no. 3, pp. 344-353, Mar. 1996.
- [2] N. K. Verghese and D. J. Allstot, "Computer-aided design consideration for mixed-signal coupling in RF integrated circuits," *IEEE J. Solid-State Circuits*, vol. 33, no. 3, pp. 314-323, Mar. 1998.
- [3] E. Charbon, R. Gharpurey, R.G. Meyer, and A. Sangiovanni-Vincentelli, "Substrate optimization based on semi-analytical techniques," *IEEE Trans. Computer-Aided Design*, vol. 18, no. 2, pp. 172-190, Feb. 1999.
- [4] M. van Heijningen, J. Compier, P. Wambacq, S. Donnay, M. Engels, and I. Bolsens, "Analysis and experimental verification of digital substrate noise generation for epi-type substrates," *IEEE J. Solid-State Circuits*, vol. 35, no. 7, pp. 1002-1008, July 2000.
- [5] E. Schrik and N.P. van der Meijs, "Combined BEM/FEM substrate resistance modeling," *Proc. Design Automation Conf.*, New Orleans, Louisiana, June 10-14, 2002.
- [6] A. Odabasioglu, M. Celik, and L. T. Pilleggi, "PRIMA: passive reduced-order interconnect macromodeling algorithm," *IEEE Tran. Computer-Aided Design*, vol. 17, no. 8, pp. 645-654, Aug. 1998
- [7] A. Samavedam, A. Sadate, K. Mayaram and T. Fiez, "A scalable substrate noise coupling model for design of mixed-signal IC's," *IEEE J. Solid-State Circuits*, vol. 35, no. 6, pp. 895-904, June 2000.
- [8] D. Ozis, T. Fiez, and K. Mayaram, "A comprehensive geometry-dependent macromodel for substrate noise coupling in heavily doped CMOS processes," *Proc. IEEE Custom Integrated Circuits Conf.*, Orlando, Florida, May 12-15, 2002, pp. 497-500.
- [9] K. H. To, P. Welch, S. Bharatan, H. Lehning, T. L. Huynh, R. Thoma, D. Monk, W.M. Huang, and V. Ilderem, "Comprehensive study of substrate noise isolation for mixed-signal circuits," *Digest. Electron Devices Meeting*, Washington, DC, Dec 2-5, 2001, pp. 22.7.1-22.7.4
- [10] H. Hasegawa, M. Furukawa and H. Yanai, "Properties of microstrip line on Si-SiO<sub>2</sub> system," *IEEE Trans. Microwave Theory Tech.*, vol. 19, no. 11, pp. 869-881, Nov. 1971.
- [11] J. Zheng, Y.-C. Hahm, V.K. Tripathi, and A. Weisshaar, "CAD-Oriented equivalent-circuit modeling of on-chip interconnects on lossy silicon substrate," *IEEE Trans. Microwave Theory Tech.*, vol. 48, no. 9, pp. 1443-1451, Sep. 2000.
- [12] A. Deutsch *et al.*, "Frequency-dependent crosstalk simulation for on-chip interconnections," *IEEE Trans. Advanced Packaging*, vol. 22, no. 8, pp. 292-308, Aug. 1999.
- [13] M. Badaroglu *et al.*, "Methodology and experimental verification for substrate noise reduction in CMOS mixed-signal ICs with synchronous digital circuits", *Proc. Solid-State Conf.*, San Francisco, CA, Feb. 4-6, 2002, 16.6.